

# Ion-beam-directed self-organization of conducting nanowire arrays

M. Batzill,\* F. Bardou,<sup>†</sup> and K. J. Snowdon<sup>‡</sup>

*Centre for Nanoscale Science and Technology, University of Newcastle, Newcastle upon Tyne NE1 7RU, United Kingdom*

(Received 2 March 2001; published 30 May 2001)

Glancing-incidence ion-beam irradiation has been used both to ease kinetic constraints which otherwise restrict the establishment of long-range order and to impose external control on the orientation of nanowire arrays formed during stress-field-induced self-ordering of calcium atoms on a  $\text{CaF}_2(111)$  surface. The arrays exhibit exceptional long-range order, with the long axis of the wires oriented along the azimuthal direction of ion-beam incidence. Transport measurements reveal a highly anisotropic electrical conductivity, whose maximum lies in the direction of the long axis of the 10.1-nm-period calcium wires.

DOI: 10.1103/PhysRevB.63.233408

PACS number(s): 68.35.Bs, 61.80.Jh, 68.65.-k, 81.40.Wx

Efficient molecular-scale patterning and long-range order are prerequisites for many potential applications of nanostructures. Self-organization phenomena<sup>1</sup> offer an attractive fabrication route, but kinetic, entropic, and steric constraints can lead to poor long-range order. Examples of self-organization phenomena in two-dimensional systems include spin-charge density modulations in high-temperature superconducting cuprate materials,<sup>2,3</sup> aligned lamellae in crystallized thin-film block copolymers,<sup>4</sup> and stress-field-related<sup>5,6</sup> dot and stripe domain structures in thin films of lattice-mismatched materials.<sup>7,8</sup> Stoichiometric ion-beam etching of surfaces is also known to induce zero-<sup>9</sup> and one-dimensional surface patterning. In particular, ripple structures have been reported, both along preferred crystallographic directions and oriented normal and parallel to the azimuthal incidence direction of ion beams used to irradiate one-component metal<sup>10–13</sup> and semiconductor<sup>14,15</sup> single-crystal surfaces at off-normal angles of incidence. Their formation is believed to be related either to competition between erosion and kinetic restrictions on the diffusion of adatoms,<sup>10–13,15</sup> or to a surface instability arising from a surface-curvature-dependent sputter yield.<sup>14,16</sup> In contrast, we report in this paper the formation of nanowire arrays by depletion of one constituent of the surface layers of an ionic crystal. As in epitaxial growth studies, strain fields associated with lattice mismatch at the interface of the resulting dissimilar materials could be expected to have an important, even dominating influence on the evolution of the surface morphology. Indeed, our experiments provide strong evidence that stress fields dominate the evolution and long-range ordering of the ripple structures we observe, the explanation of which thus differs from that reported previously. Our work illustrates that ion-beam irradiation can ease kinetic constraints restricting the establishment of long-range order in a one-dimensional self-organized system. Furthermore, the technique we describe provides a means to arbitrarily control the orientation of wirelike structures.

The calcium fluoride samples we used were cleaved under ambient conditions and rapidly transferred into an ultrahigh-vacuum chamber for ion-beam irradiation. Calcium fluoride has a crystal repeat unit  $\text{F}^- - \text{Ca}^{2+} - \text{F}^-$ . Cleavage occurs in the (111) plane between two fluorine layers, leading to a fluorine-terminated surface. Contact-mode ambient atomic force microscopy (AFM) on such surfaces revealed large

atomically flat terraces and occasional cleavage steps. Steps of one or a multiple of the Ca-Ca interlayer spacing (0.315 nm) separate individual terraces. The samples were irradiated with a 4.5 keV  $\text{Ar}^+$  ion beam under grazing angles of incidence from  $4^\circ$  to  $16^\circ$  to the surface plane and to ion fluences up to  $10^{16}$  ions/mm<sup>2</sup>. These irradiation conditions correspond to fluences up to 1500 incident  $\text{Ar}^+$  ions per surface atom and surface normal energies of the ion beam from 22 to 340 eV. After irradiation, the samples were again examined using contact-mode AFM under ambient conditions.

In a first set of experiments, the samples were continuously rotated about their surface normal during irradiation. For an ion-beam glancing angle up to  $\sim 10^\circ$ , nanometer-scale, elongated, meandering, and sometimes ramified islands of height  $\sim 0.6$  nm appear [Fig. 1(a)]. The island structures exhibit a relatively uniform width and a preferred separation of  $\sim 10$  nm, but no long-range order is apparent. At larger glancing angles ( $10^\circ$ – $16^\circ$ ), the elongation and the preferential structure size and separation disappear, and the surface becomes rough.

The observations at small glancing angles are consistent with preferential potential sputtering<sup>17</sup> of fluorine atoms, leading to a calcium-enriched surface and ultimately to segregation of calcium islands on a surface terminated by either  $\text{F}^-$  or color centers.<sup>18</sup> The estimated island heights, widths, and separations correspond to the formation of 2 ML (monolayer) high, 0.5 ML coverage structures via reconstruction of the fluorine-depleted outer  $\text{F}^- - \text{Ca}^{2+} - \text{F}^-$  trilayer of the  $\text{CaF}_2(111)$  surface.<sup>19</sup> The formation of elongated islands following ion-beam-irradiation-induced fluorine depletion is in agreement with our previous observations on this system where fluorine was eroded using low-energy electrons.<sup>20</sup> In those studies we found that a shape transition occurs, from compact to elongated islands, if the calcium adislands reach a critical size. This shape transition was interpreted as a stress relief mechanism, proposed by Tersoff and Tromp<sup>21</sup> and reported in other systems.<sup>22</sup> The formation of elongated islands itself provides a hint of a strain-induced island morphology. Furthermore, the observed preferential separation of the islands can be understood in terms of a local self-ordering of elongated domain structures on lattice-mismatched systems<sup>23</sup> (the lattice constant of calcium is  $\sim 2\%$  larger than that of  $\text{CaF}_2$ ). Such ordering demands a large calcium atom mobility. The fact that we only observe

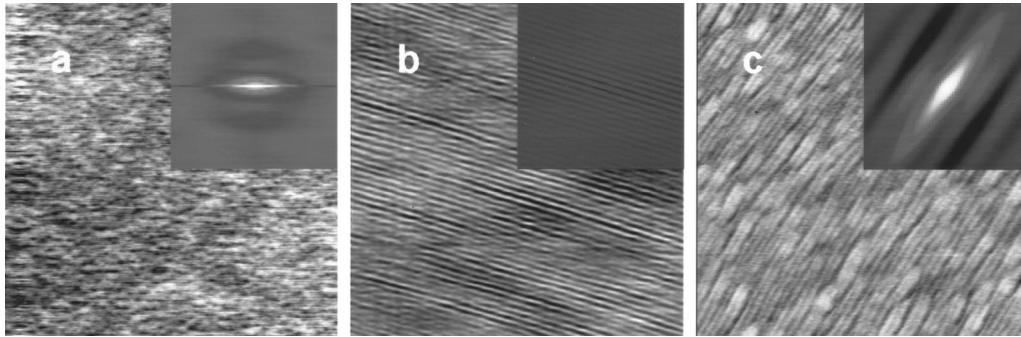


FIG. 1. Contact-mode atomic force microscope (AFM) images and corresponding autocorrelation (AC) images of cleaved  $\text{CaF}_2(111)$  surfaces following 4.5 keV  $\text{Ar}^+$  irradiation: (a) glancing angle  $10^\circ$ , fluence  $1.3 \times 10^{15}$  ions/ $\text{mm}^2$ , continuous azimuthal variation (AFM image size  $390 \times 390$  nm $^2$ , AC image size  $49 \times 49$  nm $^2$ ); (b) glancing angle  $10^\circ$ , fluence  $2.6 \times 10^{15}$  ions/ $\text{mm}^2$ , fixed azimuth (AFM image size  $540 \times 540$  nm $^2$ , AC image size  $270 \times 270$  nm $^2$ ); (c) glancing angle  $16^\circ$ , fluence  $2.6 \times 10^{15}$  ions/ $\text{mm}^2$ , fixed azimuth (AFM image size  $520 \times 520$  nm $^2$ , AC image size  $65 \times 65$  nm $^2$ ).

local ordering in this system implies that kinetic restrictions exist under these irradiation conditions. The rougher, disordered surfaces observed at larger glancing angles are consistent with the onset of kinetic sputtering, which has the potential to create pinning defects and thereby reduce the mobility of surface atoms.

We next explored the possibility that ion-beam irradiation might be used to positively influence the surface atom mobility and even remove the kinetic restrictions that prevent the development of long-range order in this system. This was achieved by holding the samples fixed during irradiation. Ambient AFM measurements on those samples revealed the formation of *periodic arrays of parallel straight nanowires*<sup>24</sup> [Fig. 1(b)]. The best arrays were formed by irradiating the samples at a glancing angle  $\sim 10^\circ$  to a fluence  $\sim 3 \times 10^{15}$  ions/ $\text{mm}^2$ . The wires were always found to be parallel to the projection of the ion beam on the sample surface; the orientation of the underlying  $\text{CaF}_2$  crystal was found to be unimportant. The crucial role of the azimuthal direction of ion-beam incidence was confirmed by the following experiment. We first irradiated a sample along an arbitrary, but fixed, direction, and observed that wires were formed along that direction. We then irradiated the same sample along a new direction, and observed that the wire orientation changed to that of the second irradiation. Irradiation under glancing angles considerably in excess of  $10^\circ$  [e.g.,  $16^\circ$  in Fig. 1(c)] led to the creation of structures that appear less ordered and rougher than those obtained at lower angles, but which nevertheless exhibit a preferential island elongation along the azimuthal direction of beam incidence.

A more quantitative measure of the extent of structure ordering in these images can be obtained from the corresponding autocorrelation images (insets to Fig. 1). The autocorrelation images of samples that have been rotated during irradiation reveal an anisotropy that is related to AFM-tip-induced material transport in the “fast” scan direction of the tip (horizontal direction in Fig. 1). However, we do see clear evidence for a preferred structure separation in the “slow” scan direction in the autocorrelation image. The corresponding cross section [Fig. 2(a)] reveals a single oscillation corresponding to a typical separation between islands of  $\sim 10$  nm. As in a glassy state, there is only short-range self-

ordering of the system under these irradiation conditions. However, if the sample is held fixed during irradiation, the autocorrelation image changes dramatically [insets to Figs. 1(b) and 1(c) and Figs. 2(b) and 2(c)]. Under ideal conditions [glancing angle  $\sim 10^\circ$ ; Figs. 1(b) and 2(b)], the autocorrelation image is not only periodic in the surface direction perpendicular to the wire axis (period 10.1 nm), but it exhibits a remarkable degree of coherence, with at least 50 oscillations visible in some images. We also observe perfect wire alignment under these conditions, over the largest areas we can scan with our AFM ( $2 \times 2$   $\mu\text{m}^2$ ). This very strong orientational anisotropy is particularly visible in the corresponding

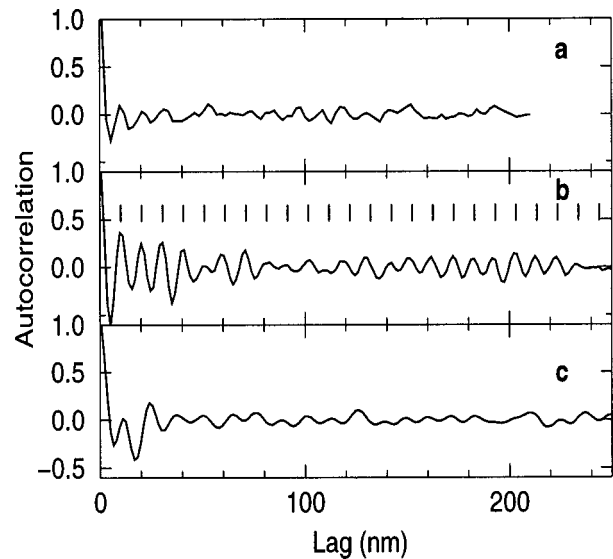


FIG. 2. Cross sections of the autocorrelation images shown in Fig. 1: (a) integrated over a vertical band of width 23 nm in the center of the AC image in Fig. 1(a); (b) integrated over a band of width 211 nm oriented normal to the long axis of the wires in Fig. 1(b) (the “beating” effect is caused by a global image distortion, which leads to an apparent dephasing followed by a reappearance of the modulation at larger lag); (c) integrated over a band of width 81 nm oriented normal to the long axis of the wires in Fig. 1(c). The tick marks in (b) are separated by 10.1 nm, the wire array periodicity.

two-dimensional (2D) Fourier spectra, whose components are concentrated in a  $1^\circ$  sector (full width). Autocorrelation images of samples that have been held fixed during irradiation under higher glancing angles [e.g.,  $16^\circ$ ; Figs. 1(c) and 2(c)] reveal ordering which is longer range than that for rotated samples [e.g., Figs. 1(a) and 2(a)], but shorter range than that observed for samples prepared under more ideal conditions [e.g., Figs. 1(b) and 2(b)]. The 2D Fourier spectra, corresponding for example to the image in Fig. 1(b), now extend over a  $10^\circ$  sector (full width).

These results suggest the following mechanism for wire array formation. Potential sputtering under glancing-incidence ion-beam irradiation is known to lead to local self-ordering of the fluorine-depleted  $\text{CaF}_2(111)$  surface into elongated nanosized calcium stress domains.<sup>19</sup> These stress domains arise from an attempt by the system to achieve coherent calcium island (wire) growth on top of the  $\text{CaF}_2$  substrate, despite the latter possessing a 2% larger lattice constant. This results in compressively stressed  $\text{CaF}_2$  layers underneath the calcium wires and tensile stressed areas between the wires. The competition between minimizing the length of domain boundaries (wire edges), which drives coarsening, and the reduction of strain energy, which favors refinement of the wires, results in long-range structural order. The lowest-energy pattern for such a stress field is a periodic array of straight stripes,<sup>23,25</sup> which we succeed in obtaining by not rotating the sample during irradiation. If the sample is rotated, the time-averaged surface mobility is isotropic and the system achieves only short-range order, as is indeed typical of two-phase systems.<sup>1</sup> Kinetic restrictions prevent the onset of long-range ordering. When the sample is held fixed during irradiation, a combination of forward-directed (anisotropic) momentum transfer to exposed surface atoms, shadowing, sputtering of atoms on exposed sections of a meandering wire, and energy minimization criteria (minimization of the domain wall energy) all combine to aid formation of *macroscopically long, straight wires*. Glancing-incidence ion-beam irradiation along a fixed azimuth is the external factor that assists the lattice-mismatch-induced local stress fields achieve global energy minimization and macroscopic long-range order. As expected, if the glancing angle of irradiation is too large, pinning defects are created in the surface and kinetic restrictions again prevent the establishment of long-range order.

Our surface erosion model implies that the islands and nanowires are composed of calcium. As bulk calcium is an electrical conductor, we felt that the nanowires may themselves conduct, and if so we would expect samples such as that imaged in Fig. 1(b) to exhibit an extremely anisotropic surface conductivity. To check that possibility, we fabricated arrays like that shown in Fig. 1(b) and on these evaporated a pair of silver contacts separated by a gap of  $10\text{ }\mu\text{m}$  in length and  $200\text{ }\mu\text{m}$  in width. We used the same electrode geometry on different samples to measure the surface conductivity, in vacuum, both along and perpendicular to the wire axis. Along the wires, we obtained conductances in the range of  $(1-6)\times 10^{-8}\text{ }\Omega^{-1}$  exhibiting Ohmic characteristics. Conductances less than  $4\times 10^{-11}\text{ }\Omega^{-1}$  (our sensitivity threshold) are measured perpendicular to the wires and on unirradiated samples. These measurements strongly support our interpretation that the nanowires are composed of calcium and that their length is at least of the order of the gap between the contacts ( $10\text{ }\mu\text{m}$ ).

We have shown that glancing-incidence ion-beam irradiation can be used to simultaneously eliminate kinetic constraints and impose external control on the orientation of stripe domains formed during stress-field-induced self-ordering of a fluorine-depleted calcium layer on a  $\text{CaF}_2(111)$  surface. We have achieved exceptional long-range two-dimensional order of molecular-width wires. The ion beam may either be suppressing meandering elongated island growth via kinetic sputtering of projecting atoms or introducing an anisotropy in the diffusion of surface atoms. Either way, it seems probable that glancing-incidence ion beams could also be used to fix the orientation of quasi-one-dimensional structures and perhaps even the lattice order and orientation of quasi-zero-dimensional structures in lattice-mismatched systems grown by molecular-beam epitaxy and other material-deposition techniques. Such highly coherent nanowire arrays may possess unusual ac conductivity and optical properties<sup>26,27</sup> and offer exciting possibilities in atom optics and as nanostructured templates for the growth of inorganic and biological materials.

The loan of equipment by the Institute for Surface Modification, Leipzig, is gratefully acknowledged. F.B. is financially supported by the Centre National de la Recherche Scientifique, France.

\*Present address: Department of Chemistry, University of Southern California, Los Angeles, CA 90089-0482.

†Permanent address: IPCMS, UMR 46 CNRS, F-67037 Strasbourg Cedex, France.

‡Corresponding author. Electronic address: k.j.snowdon@ncl.ac.uk

<sup>1</sup>M. Seul and D. Andelman, *Science* **267**, 476 (1995).

<sup>2</sup>T. Noda, H. Eisaki, and S. Uchida, *Science* **286**, 265 (1999).

<sup>3</sup>X. J. Zhou, P. Bogdanov, S. A. Kellar, T. Noda, H. Eisaki, S. Uchida, Z. Hussain, and Z.-X. Shen, *Science* **286**, 268 (1999).

<sup>4</sup>G. Reiter, G. Castelein, P. Hoerner, G. Riess, A. Blumen, and J.-U. Sommer, *Phys. Rev. Lett.* **83**, 3844 (1999).

<sup>5</sup>H. Ibach, *Surf. Sci. Rep.* **29**, 193 (1997).

<sup>6</sup>K. Pohl, M. C. Bartelt, J. de la Figuera, N. C. Bartelt, J. Hrbek,

and R. Q. Hwang, *Nature (London)* **397**, 238 (1999).

<sup>7</sup>M. Grundmann *et al.*, *Phys. Rev. Lett.* **74**, 4043 (1995).

<sup>8</sup>G. Springholz, V. Holy, M. Pinczolis, and G. Bauer, *Science* **282**, 734 (1998).

<sup>9</sup>S. Facsko, T. Dekorsy, C. Koerdert, C. Trappe, H. Kurz, A. Vogt, and H. L. Hartnagel, *Science* **285**, 1551 (1999).

<sup>10</sup>S. Rusponi, G. Costantini, C. Boragno, and U. Valbusa, *Phys. Rev. Lett.* **81**, 4184 (1998).

<sup>11</sup>S. Rusponi, C. Boragno, and U. Valbusa, *Phys. Rev. Lett.* **78**, 2795 (1997).

<sup>12</sup>S. Rusponi, G. Costantini, C. Boragno, and U. Valbusa, *Phys. Rev. Lett.* **81**, 2735 (1998).

<sup>13</sup>S. Rusponi, G. Costantini, F. Buatier de Mongeot, C. Boragno,

- and U. Valbusa, Appl. Phys. Lett. **75**, 3318 (1999).
- <sup>14</sup>E. Chason, T. M. Mayer, B. K. Kellerman, D. T. McIlroy, and A. J. Howard, Phys. Rev. Lett. **72**, 3040 (1994).
- <sup>15</sup>J. Erlebacher, M. J. Aziz, E. Chason, M. B. Sinclair, and J. A. Floro, Phys. Rev. Lett. **82**, 2330 (1999).
- <sup>16</sup>R. Cuerno and A.-L. Barabási, Phys. Rev. Lett. **74**, 4746 (1995).
- <sup>17</sup>P. Williams, Phys. Rev. B **23**, 6187 (1981).
- <sup>18</sup>U. O. Karlsson, F. J. Himpsel, J. F. Morar, F. R. McFeely, D. Rieger, and J. A. Yarmoff, Phys. Rev. Lett. **57**, 1247 (1986).
- <sup>19</sup>M. Batzill, F. Bardou, and K. J. Snowdon, Phys. Rev. Lett. **85**, 780 (2000).
- <sup>20</sup>M. Batzill and K. J. Snowdon, Appl. Phys. Lett. **77**, 1955 (2000).
- <sup>21</sup>J. Tersoff and R. M. Tromp, Phys. Rev. Lett. **70**, 2782 (1993).
- <sup>22</sup>B. Müller, L. Nedelmann, B. Fischer, H. Brune, J. V. Barth, and K. Kern, Phys. Rev. Lett. **80**, 2642 (1998).
- <sup>23</sup>P. Zeppenfeld, M. Krzyzowski, Ch. Romainczyk, G. Comsa, and M. G. Lagally, Phys. Rev. Lett. **72**, 2737 (1994).
- <sup>24</sup>M. Batzill, F. Bardou, and K. J. Snowdon, UK patent application 9901655.2 (1999).
- <sup>25</sup>K.-O. Ng and D. Vanderbilt, Phys. Rev. B **52**, 2177 (1995).
- <sup>26</sup>J. B. Pendry, A. J. Holden, W. J. Stewart, and I. Youngs, Phys. Rev. Lett. **76**, 4773 (1996).
- <sup>27</sup>W. A. de Heer, A. Chatelain, and D. Ugarte, Science **268**, 845 (1995).